

Signatures of the Baryon Acoustic Oscillations on the Convergence Power Spectrum of Weak lensing by Large Scale Structure

Tong-Jie Zhang^{a,b,*} Qiang Yuan^c Tiang Lan^a

^a*Department of Astronomy, Beijing Normal University, Beijing, 100875, P.R.China*

^b*Kavli Institute for Theoretical Physics China, Institute of Theoretical Physics, Chinese Academy of Sciences (KITPC/ITP-CAS), P.O.Box 2735, Beijing 100080, P.R. China*

^c*Key Laboratory of Particle Astrophysics, Institute of High Energy Physics, Chinese Academy of Sciences, P.O.Box 918-3, Beijing 100049, P.R.China*

Abstract

We employ an analytical approach to investigate the signatures of Baryon Acoustic Oscillations (BAOs) on the convergence power spectrum of weak lensing by large scale structure. It is shown that the BAOs wiggles can be found in both of the linear and nonlinear convergence power spectra of weak lensing at about $40 \leq l \leq 600$, but they are weaker than that of matter power spectrum. Although the statistical error for LSST are greatly smaller than that of CFHT and SNAP survey especially at about $30 < l < 300$, they are still larger than their maximum variations of BAOs wiggles. Thus, the detection of BAOs with the ongoing and upcoming surveys such as LSST, CFHT and SNAP survey confront a technical challenge.

Key words: cosmology: theory, gravitational lensing, large-scale structure of universe

1 Introduction

In the early universe prior to recombination, the free electrons couple the baryons to the photons through Coulomb and Compton interactions, so these

* Corresponding author.

Email address: tjzhang@bnu.edu.cn (Tong-Jie Zhang).

three species move together as a single fluid. The primordial cosmological perturbations on small scales excite sound waves in this relativistic plasma, which results in the pressure-induced oscillations and acoustic peak (Bond & Efstathiou, 1984; Eisenstein & Hu, 1998). The memory of these baryon acoustic oscillations (BAOs) still remain after the epoch of recombination. The BAOs leave their imprints through the propagating of photons on the last scattering surface and produce a harmonic series of maxima and minima in the anisotropy power spectrum of the cosmic microwave background (CMB) at $z \approx 1000$. In addition, due to the significant fraction of baryons in the universe, BAOs can also be imprinted onto the late-time power spectrum of the non-relativistic matter (Bond & Efstathiou, 1984; Hu & Sugiyama, 1996; Eisenstein & Hu, 1998), which have been detected in the large-scale correlation function of Sloan Digital Sky Survey (SDSS) luminous red galaxies (Eisenstein, 2005), and the power spectrum of 21 cm emission generated from the neutral hydrogen from the epoch of reionization through the underlying density perturbation (Mao & Wu, 2008; Chang et al., 2008). Essentially, the BAOs can give rise to the wiggles in the matter power spectrum of large scale structure during the evolution of the universe. Gravitational lensing can directly reveal the strength of gravitational clustering (Pen et al., 2003; Chen, 2005), and weak gravitational lensing is the direct measurement of the projected mass distribution of the large-scale structure (Mellier, 1999; Bartelmann & Schneider, 2001; Refregier, 2003; Lewis & Challinor, 2006; Munshi et al., 2008). Therefore, the BAOs prior to recombination should also be imprinted onto weak lensing power spectrum. Recently, the influence of baryons on the weak lensing power spectrum are investigated by many works (White, 2004; Zhan & Knox, 2004; Jing et al., 2006). Zhang (2008) study self calibration of galaxy bias in spectroscopic redshift surveys of baryon acoustic oscillations to show that SKA is able to detect BAO in the velocity power spectrum, and the precision measurement of cosmic magnification are also demonstrated (Zhang & Pen, 2005, 2006). The ongoing and upcoming surveys such as the Canada-France-Hawaii-Telescope (CFHT) Legacy Survey¹, the SuperNova Acceleration Probe² (SNAP) and the Large Synoptic Survey Telescope³ (LSST) will significantly reduce the statistical errors to a few percent level in the measurement of weak lensing power spectrum. Therefore, it is necessary to explore the feasibility of detecting the BAOs in weak lensing surveys. In this paper, we concentrate on the wiggles of BAOs on the power spectrum of weak lensing by large scale structure and their detectability for current weak lensing survey.

¹ <http://www.cfht.hawaii.edu/Science/CFHLS/>

² <http://snap.lbl.gov>: SNAP is being proposed as part of the Joint Dark Energy Mission (JDEM)

³ <http://www.lsst.org>

2 Matter Power Spectra

We express the linear matter power spectrum in dimensionless form as the variance per unit logarithmic interval in wavenumber ($\log_{10} k$)

$$\Delta^2(k, z) = \frac{k^3 P(k, z)}{2\pi^2} = \delta_H^2 \left(\frac{k}{H_0} \right)^{3+n_s} T^2(k) \frac{D^2(z)}{D^2(0)} \quad (1)$$

where $T(k)$ and $D(z)$ are transfer function and linear growth factor respectively. We consider the effect of baryon content (thereby BAOs), so the transfer function $T(k)$ can be approximately separated into the cold dark matter (CDM) and baryon components: $T(k) = (\Omega_b/\Omega_m)T_b(k) + (\Omega_c/\Omega_m)T_c(k)$, where Ω_c is the CDM density parameter at present, $\Omega_c = \Omega_m - \Omega_b$. We adopt the asymptotic solutions to both $T_b(k)$ and $T_c(k)$ near the sound horizon given by Eisenstein & Hu (1998). For convenience, we employ the widely used fitting formula, which are calibrated with N-body simulation and given by Peacock & Dodds (1996), to map the linear matter power spectrum to the nonlinear power spectrum. Throughout this paper, we employ a concordance cosmological model revealed by the WMAP five-year observations (Hinshaw, 2008): $\Omega_m = 0.258$, $\Omega_\Lambda = 0.742$, $\Omega_b = 0.044$, $h = 0.719$, $n_s = 1$.

Mao & Wu (2008) revealed that the signatures of BAOs, i.e., wiggles, are seen at wavenumber $k \sim 0.1 h\text{Mpc}^{-1}$ in both of the linear and nonlinear matter power spectra with the inclusion of baryons at relatively high redshift $z=6$ when cosmic reionization ends. Due to different purpose, we in Fig.1 plot the matter power spectra for three different matter contents: pure CDM (dashed line), pure baryons (dotted line) and mixed baryons+CDM (solid line) but at redshift $z=2, 1, 0.5$ and 0 respectively. The black lines correspond to the nonlinear power spectra of matter, while the red ones are the linear power spectra. In both of the linear and nonlinear power spectra of mixed baryons+CDM, the BAOs wiggles are clearly seen at wavenumber $k \sim 0.1 h\text{Mpc}^{-1}$. It is also shown that, with the decrease of redshift, the clustering of structures are enhanced for both of pure CDM and mixed baryons+CDM models. Compared with pure CDM case, the mixed baryons+CDM case can suppress the linear and nonlinear power spectrum by an order of a few percents or more at about $k \geq 0.1 h\text{Mpc}^{-1}$. For clarity, we demonstrate the first derivative of power spectrum $\log_{10} \Delta^2(k)$ with respect to $\log_{10} k$ for pure CDM (dashed line) and mixed baryons+CDM (solid line) at redshift $z=2, 1, 0.5$ and 0 respectively in Fig.2. The minimum here correspond to the maximum in Fig.1, and about three wiggles are clearly revealed with the inclusion of baryon contents. We also see that, compared with linear power spectrum (red solid line), the nonlinear evolution of structure (black solid line) can suppress the amplitude of BAOs wiggles and shift them to small scales with decrease of redshift. To

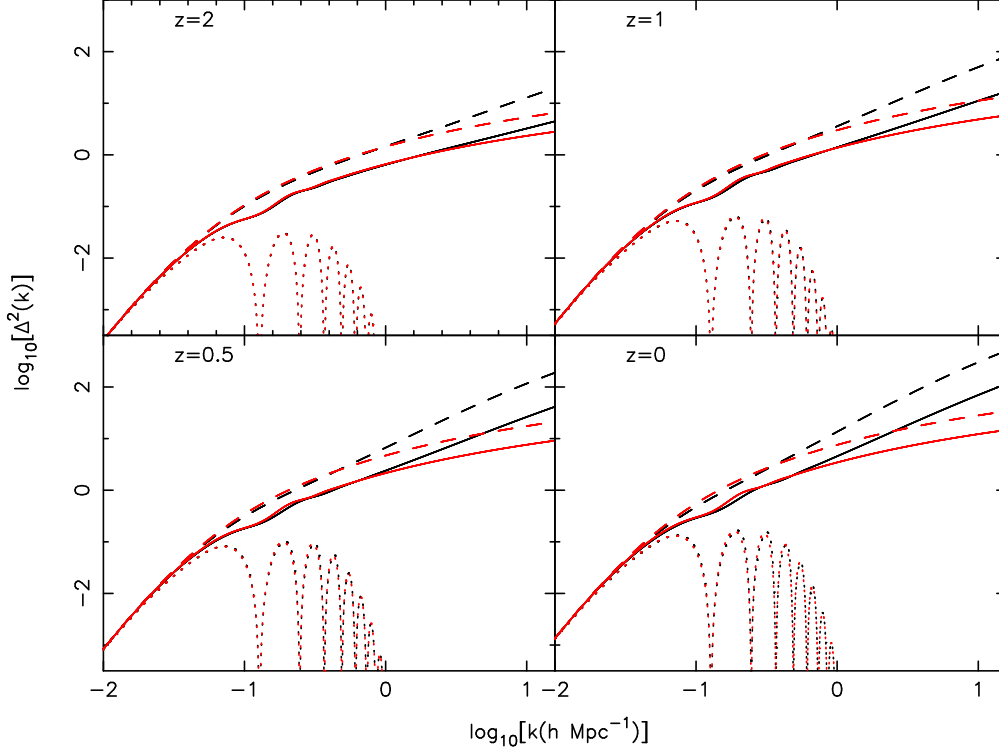


Fig. 1. Matter power spectra for three different matter contents: pure CDM (dashed line), pure baryons (dotted line) and mixed baryons+CDM (solid line) at redshift $z=2, 1, 0.5$ and 0 respectively. The black lines correspond to the nonlinear power spectra of matter, while the red ones the linear power spectra.

further show the effect of BAOs, we plot the ratio of power spectrum for the mixed baryons+CDM to that for pure CDM at redshift $z=2, 1, 0.5$ and 0 respectively in Fig.3. The solid and dashed lines correspond to the ratios of nonlinear and linear power spectra respectively. Similar to Fig.2, the wiggles for both of linear and nonlinear power spectrum are also seen clearly. Except for at the scales (l) around wiggles, the suppression on the amplitude of nonlinear power spectrum due to the inclusion of baryon contents increase with the decrease of scales, while that for linear power spectrum increase slightly. Thus, the BAOs signatures can be imprinted onto the entire history of cosmic structure evolution since the epoch of recombination.

3 Weak Lensing Convergence Power Spectrum

Through the matter power spectrum, BAOs signature enters into the statistics of weak lensing by large scale structure. Using Limber's approximation(Kaiser, 1992; Bartelmann & Schneider, 2001; Simon, 2007), we can write the conver-

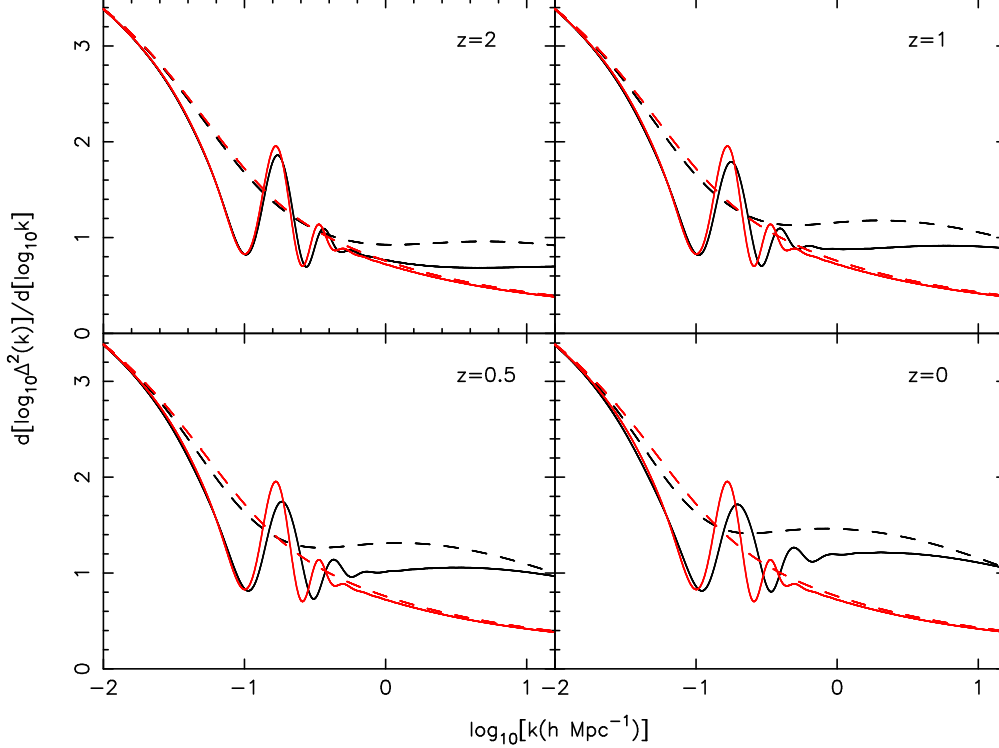


Fig. 2. The first derivative of power spectrum $\log_{10} \Delta^2(k)$ with respect to $\log_{10} k$ for pure CDM (dashed line) and mixed baryons+CDM (solid line) at redshift $z=2, 1, 0.5$ and 0 respectively. The black lines correspond to the nonlinear power spectra of matter, while the red ones the linear power spectra.

gence power spectrum of weak lensing as

$$C_l = \int_0^{\chi_s} d\chi \frac{W^2(\chi)}{r^2(\chi)} P(l/r(\chi), z) \quad (2)$$

where $r(\chi)$ is the radial comoving coordinate distance and $r(\chi) = \sinh(\chi)$ for open, $r(\chi) = \chi$ for flat and $r(\chi) = \sin(\chi)$ for closed geometry of Universe respectively. The weight function $W(\chi) = \frac{3}{2} \Omega_m H_0^2 g(\chi)(1+z)$ is determined by the source galaxy distribution function $n(z)$ and the lensing geometry $g(\chi) = r(\chi) \int_{\chi}^{\infty} d\chi' n(\chi') \frac{r(\chi' - \chi)}{r(\chi')}$. Here $n(z) = n(\chi) d\chi/dz$ is normalized such that $\int_0^{\infty} n(z) dz = 1$. If all sources are at a single redshift z_s (or the distribution of source galaxies is given within a thin sheet at redshift z_s), we have $n(z) = \delta(z - z_s)$ and then $g(\chi) = r(\chi)r(\chi_s - \chi)/r(\chi_s)$. Following the works (Rudd et al., 2008; Jing et al., 2006), for simplicity, we assume that the source galaxies are distributed within a thin sheet at z_s throughout this paper. For a flat universe, $d\chi = dr = dz/H(z)$, so Eq.(2) reduces to

$$C_l = \frac{2\pi^2}{l^3} \int_0^{z_s} dz \frac{W^2(z) r(z)}{H(z)} \Delta^2(l/r(z), z). \quad (3)$$

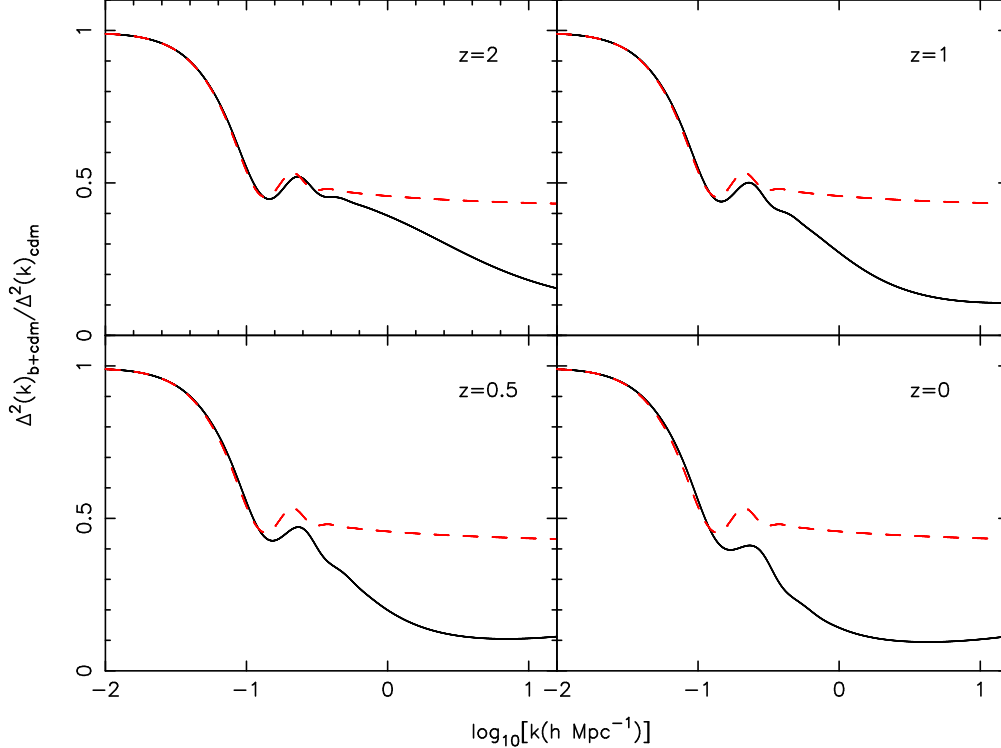


Fig. 3. The ratio of power spectrum for the mixed baryons+CDM to that for pure CDM at redshift $z=2, 1, 0.5$ and 0 respectively. The solid and dashed lines correspond to the ratios of nonlinear and linear power spectra respectively.

In Eqs.(2) and (3), the matter power spectrum as a function of wavenumber $k = l/r(z)$ and redshift z satisfies Eq.(1): $\Delta^2(l/r(z), z) = k^3 P(l/r(z), z)/2\pi^2$. In Fig.4, we show the signatures of BAOs on the convergence power spectra of weak lensing with the source galaxies at redshift $z_s = 0.5, 1.0$ and 2.0 , respectively. This figure plot the convergence power spectra $\log_{10}[l(l+l)C_l/2\pi]$ for three different matter contents: pure CDM (dashed line), pure baryons (dotted line) and mixed baryons+CDM (solid line) respectively. Both of the linear and nonlinear power spectra of weak lensing are suppressed at about $l > 10$ due to the inclusion of baryon contents. The BAOs wiggles can be visible in both of the linear and nonlinear power spectra for the mixed baryons+CDM model at about $40 \leq l \leq 600$. With the increase of z_s from 0.5 to 2 , the wiggles are shifted to small scales for both of linear and nonlinear power spectra, i.e., from the scale range of about $40 \leq l \leq 250$ to $100 \leq l \leq 600$. Compared with that of matter power spectrum, the BAOs wiggles in the convergence power spectra are weaker. To be more clearly, the first derivative of $\log_{10}[l(l+l)C_l/2\pi]$ with respect to $\log_{10} l$ and the ratio, C_l^{b+CDM}/C_l^{CDM} of power spectrum for the mixed baryons+CDM to that for pure CDM are shown in Upper panel and Bottom panel of Fig.5 respectively. At about $40 < l < 600$, the wiggles are revealed clearly in Upper panel for different z_s due to the inclusion of baryon contents. Similar to matter power spectrum (Fig.3), it is shown in Bottom panel for different z_s that the suppression on nonlinear convergence power

spectrum amplitude due to the inclusion of baryon contents increases with the decrease of scales (l) except for the scales around wiggles, while that for linear convergence power spectrum vary slightly.

4 Detectability

In order to demonstrate the detectability of BAOs, we compare our results with the statistical uncertainty in the measurement of the convergence power spectrum by ongoing and upcoming weak lensing survey projects such as CFHT, SNAP and LSST. The statistical errors in the measurements of weak lensing power spectrum C_l (assuming Gaussianity) are described by (Kaiser, 1992, 1998; Seljak, 1998; Huterer, 2002)

$$\Delta C_l = \sqrt{\frac{2}{(2\ell + 1)f_{\text{sky}}}} \left(C_l + \frac{\gamma_{\text{int}}^2}{\bar{n}_g} \right), \quad (4)$$

where $f_{\text{sky}} = \Theta^2\pi/129600$ is the coverage fraction of sky covered by a survey of area Θ^2 in units of deg^2 , \bar{n}_g is the effective surface number density of source galaxies with measurable shapes on the sky, and γ_{int} is the rms intrinsic shape noise for each galaxy. The cosmic variance, which corresponds to the first term of Eq.(4), dominates the uncertainty in the observed convergence power spectrum on large scales, and Poisson noise corresponding to the second term come from the limited number of galaxies on small scales. As an ongoing observational project, we consider a survey CFHT which covers a fraction $f_{\text{sky}} = 4 \times 10^{-3}$ of the sky, with a number density of source galaxies of $\bar{n}_g = 13 \text{ arcmin}^{-2}$. For future survey, we take $f_{\text{sky}} = 0.5$ and $\bar{n}_g = 50 \text{ arcmin}^{-2}$ for LSST survey and $f_{\text{sky}} = 0.025$ and $\bar{n}_g = 100 \text{ arcmin}^{-2}$ for SNAP survey respectively (Rudd et al., 2008). We adopt $\gamma_{\text{int}} = 0.22$ for the variance of the intrinsic ellipticity of source galaxies. The top panel of Fig.6 shows the non-linear convergence power spectra $\log_{10}[l(l+1)C_l/2\pi]$ for mixed baryons+CDM with statistical errors with the source galaxies distributed within a thin sheet at $z_s = 0.4$. For CFHT and SNAP survey, the statistical error are greatly larger than the maximum variations of wiggles, which is the power spectrum difference between wiggle peak and adjacent troughs. Compared with that of CFHT and SNAP survey, the statistical error for LSST are relatively small especially at about $30 < l < 300$. In addition, we also in the bottom panel of Fig.6 plot the signal-to-noise $C_l/\Delta C_l$ of the convergence power spectrum for the weak lensing survey projects. It is noticed that the range of scales with high signal-to-noise for LSST is much wider than that of CFHT and SNAP. Even so, it seems that a significant detection of BAOs wiggles on convergence power spectra is still difficult for current weak lensing survey due to the weakness of BAOs signals themselves and limitation of statistical errors of current

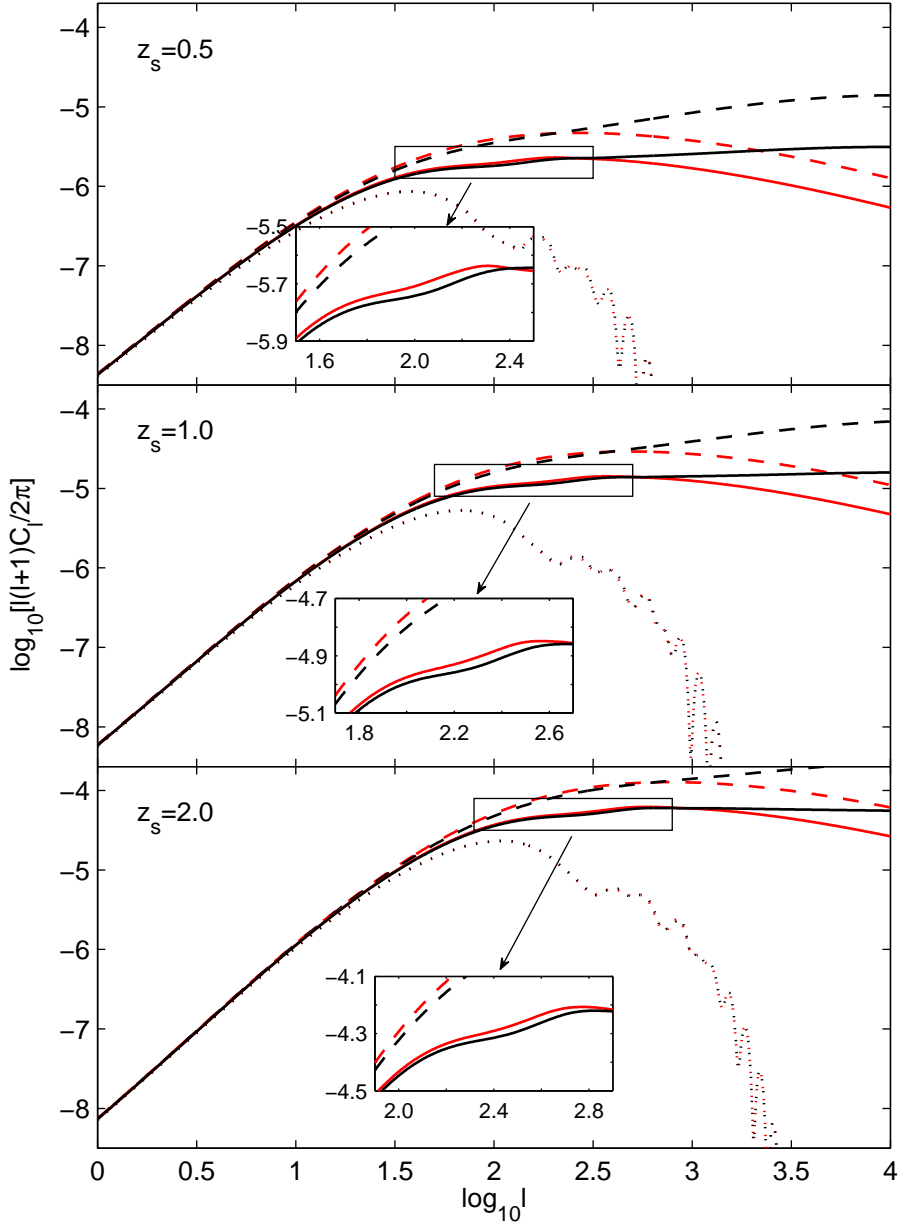


Fig. 4. The convergence power spectra $\log_{10}[l(l+l)C_l/2\pi]$ for three different matter contents: pure CDM (dashed line), pure baryons (dotted line) and mixed baryons+CDM (solid line) respectively. The black lines correspond to the nonlinear power spectra of matter, while the red ones are the linear power spectra. The inset shows an expanded view of BAOs wiggles. Here the source galaxies are distributed within a thin sheet at redshift $z_s = 0.5, 1.0$ and 2.0 , respectively.

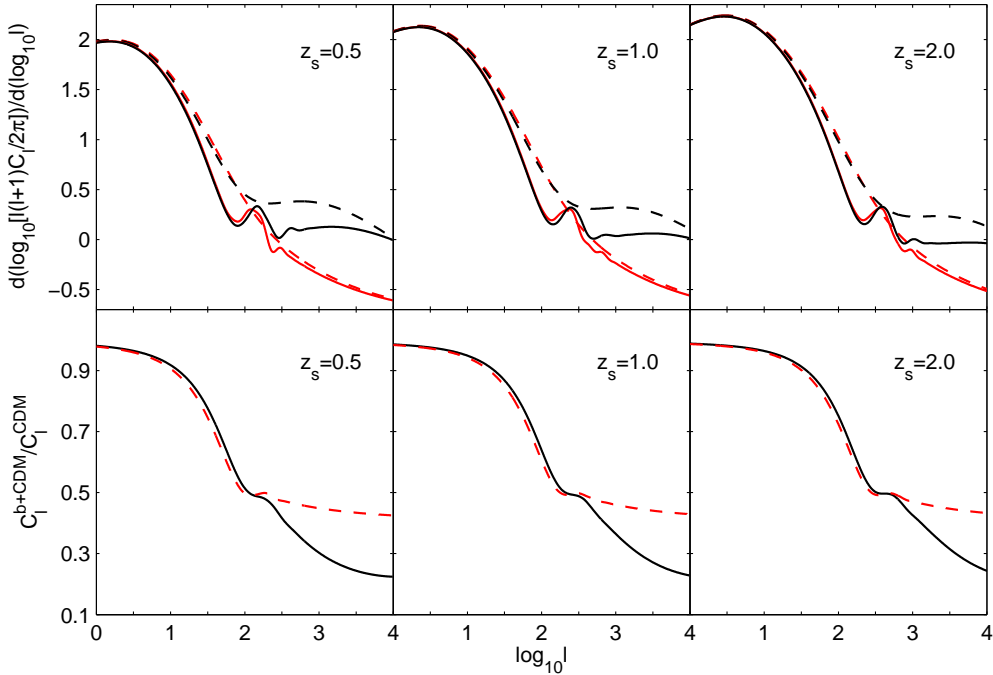


Fig. 5. *Upper panel* of each plot for different z_s : The first derivative of $\log_{10}[l(l+l)C_l/2\pi]$ with respect to $\log_{10}l$ for pure CDM (dashed line) and mixed baryons+CDM (solid line) respectively. The black lines correspond to the nonlinear power spectra of matter, while the red ones the linear power spectra. *Bottom panel* of each plot for different z_s : the ratio, C_l^{b+CDM}/C_l^{CDM} of power spectrum for the mixed baryons+CDM to that for pure CDM for the nonlinear power spectrum (black solid line) and linear power spectrum (red dashed line).

telescopes. Our result is roughly in agreement with that of work(Simpson, 2006).

5 Conclusions

In this paper, we use an analytical approach to present signatures of BAOs on the convergence power spectrum of weak lensing. We show that, in both of the linear and nonlinear matter power spectra of mixed baryons+CDM, the BAOs wiggles can be clearly seen at about $k \sim 0.1 h\text{Mpc}^{-1}$. With the decrease of redshift, the clustering of structures are enhanced for both of the pure CDM and mixed baryons+CDM models. Compared with pure CDM case, the mixed baryons+CDM case can suppress the linear and nonlinear matter power spectrum by an order of a few percents or more at about $k \geq 0.1 h\text{Mpc}^{-1}$. The nonlinear evolution of structure can suppress the amplitude of BAOs wiggles and shift them to small scales with decrease of redshift. For the convergence

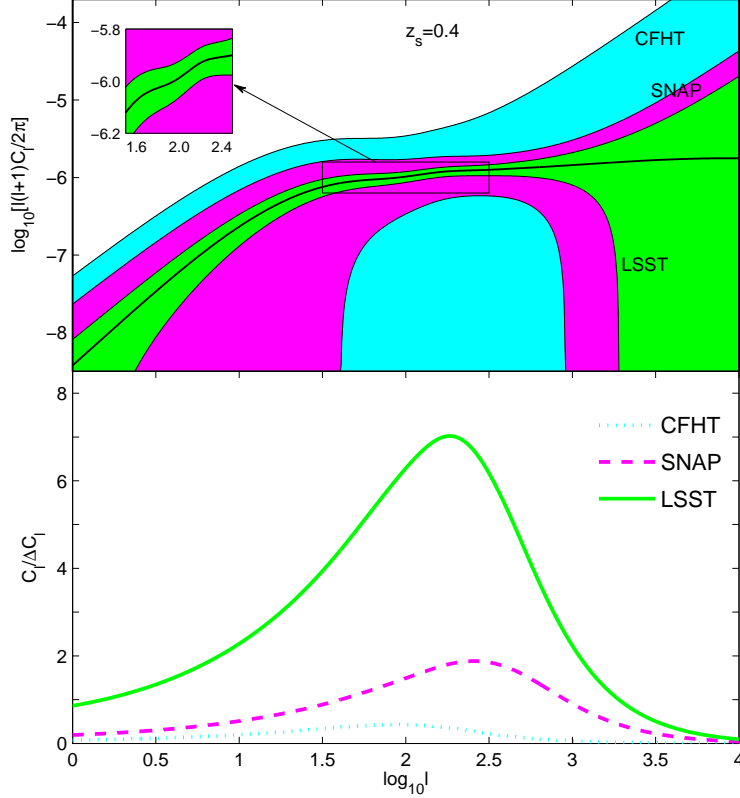


Fig. 6. *Top panel:* The nonlinear convergence power spectra $\log_{10}[l(l+1)C_l/2\pi]$ just for mixed baryons+CDM with statistical errors. The three shaded regions represent the statistical errors expected by the CFHT (cyan), SNAP (magenta), and LSST (green) from outermost to innermost bands, respectively. *Bottom panel:* The signal-to-noise $C_l/\Delta C_l$ of the convergence power spectrum for the CFHT (cyan dotted line), SNAP (magenta dashed line), and LSST (green solid line)

power spectrum of weak lensing, we show that the BAOs wiggles can be visible in both of the linear and nonlinear power spectra for the mixed baryons+CDM model at about $40 \leq l \leq 600$, but they are weaker than that of matter power spectrum. With the increase of z_s from 0.5 to 2, the BAOs wiggles are shifted to small scales for both of linear and nonlinear power spectra, i.e., from the range of about $40 \leq l \leq 250$ to $100 \leq l \leq 600$. We also study the detectability of BAOs's wiggles for weak lensing survey. Although the statistical error for LSST are greatly smaller than that of CFHT and SNAP survey especially at about $30 < l < 300$, they are still larger than the their maximum variations of BAOs wiggles. Thus, the detection of BAOs with the ongoing and upcoming surveys such as LSST, CFHT and SNAP survey i confront a technical challenge. Therefore, we expect future weak lensing survey with more lower statistical errors to capture BAOs wiggles signal from the convergence power spectrum. In addition, we have shown that the BAOs signatures can be im-

printed onto the entire history of cosmic structure evolution since the epoch of recombination. The future observation of BAOs on weak lensing will provide a complementary knowledge of current BAOs measurement. On the other hand, the BAOs provide a “standard ruler” for the determination of cosmological parameters especially the probes of dark energy, so the combination of BAOs measurement by weak lensing together with other detection of BAOs signature at different stage: the last scattering surface, reionization and large scale distribution of galaxies in local universe, will supply more robust constraint on cosmological models in the future.

Acknowledgments. We are very grateful to the anonymous referee for his valuable comments and suggestions that greatly improve this paper. We also thank Dr.Pengjie Zhang for valuable discussion and useful comment. This work was supported by the National Science Foundation of China (Grants No.10473002, 10533010), the Ministry of Science and Technology National Basic Science program (project 973) under grant No.2009CB24901 and the Scientific Research Foundation for the Returned Overseas Chinese Scholars, State Education Ministry.

References

- Bartelmann, M. & Schneider, P. 2001, *Phys. Rep.*, 340, 291
Bond, J. R. & Efstathiou, G. 1984, *ApJL*, 285, L45
Chang, T.-C., Pen, U.-L., Peterson, J. B., & McDonald, P. 2008, *Physical Review Letters*, 100, 091303
Chen, D.-M. 2005, *ApJ*, 629, 23
Eisenstein, D. J. ,et al, . 2005, *ApJ*, 633, 560
Eisenstein, D. J. & Hu, W. 1998, *ApJ*, 496, 605
Hinshaw, G. ,et al. 2008, *ArXiv e-prints*: 0803.0732
Hu, W. & Sugiyama, N. 1996, *ApJ*, 471, 542
Huterer, D. 2002, *PRD*, 65, 063001
Jing, Y. P., Zhang, P., Lin, W. P., Gao, L., & Springel, V. 2006, *ApJL*, 640, L119
Kaiser, N. 1992, *ApJ*, 388, 272
—. 1998, *ApJ*, 498, 26
Lewis, A. & Challinor, A. 2006, *Phys. Rep.*, 429, 1
Mao, X.-C. & Wu, X.-P. 2008, *ApJL*, 673, L107
Mellier, Y. 1999, *ARA&A*, 37, 127
Munshi, D., Valageas, P., van Waerbeke, L., & Heavens, A. 2008, *Phys. Rep.*, 462, 67
Peacock, J. A. & Dodds, S. J. 1996, *MNRAS*, 280, L19
Pen, U., Zhang, T., van Waerbeke, L., Mellier, Y., Zhang, P., & Dubinski, J. 2003, *ApJ*, 592, 664

- Refregier, A. 2003, *ARA&A*, 41, 645
Rudd, D. H., Zentner, A. R., & Kravtsov, A. V. 2008, *ApJ*, 672, 19
Seljak, U. 1998, *ApJ*, 506, 64
Simon, P. 2007, *A&A*, 473, 711
Simpson, F. 2006, *ApJL*, 647, L91
White, M. 2004, *Astroparticle Physics*, 22, 211
Zhan, H. & Knox, L. 2004, *ApJL*, 616, L75
Zhang, P. 2008, *ArXiv e-prints*: 0802.2416
Zhang, P. & Pen, U.-L. 2005, *Physical Review Letters*, 95, 241302
—. 2006, *MNRAS*, 367, 169